Geological Quarterly, 2022, 66: 1
DOI: http://dx.doi.org/10.7306/gq.1634

Source rock potential of the Miocene sedimentary rocks in the Carpathian Foredeep of the Czech Republic

Eva GERŠLOVÁ[1, *], Lujza MEDVECKÁ[1], Petr JIRMAN[1, 2], Slavomír NEHYBA[1] and Vladimír OPLETAL[3]

[1] Department of Geological Sciences, Faculty of Science, Masaryk University, Kotlářská 2, 611 37, Brno, Czech Republic

[2] Czech Geological Survey, branch Brno, Leitnerova 22, 602 00 Brno, Czech Republic

[3] MND a.s., Úprkova 807/6, 695 01 Hodonín, Czech Republic

Geršlová, E., Medvecká, L., Jirman, P., Nehyba, S., Opletal, V., 2022. Source rock potential of the Miocene sedimentary rocks in the Carpathian Foredeep of the Czech Republic. Geological Quarterly, 2022, 66: 1, doi: 10.7306/gq.1634

Associate Editor: Dariusz Więcław

We determine the organic matter content, its thermal maturity, genetic type, and source rock potential of the Miocene sedimentary rocks in the Czech Carpathian Foredeep. In the Czech Republic the Carpathian Foredeep represents a peripheral foreland basin formed due to the tectonic emplacement and loading of the Alpine-Carpathian Thrust Wedge onto the passive margin of the Bohemian Massif. Random vitrinite/huminite reflectance measurements and maceral analyses were performed on 25 samples from the Carpathian Foredeep succession. Additionally, results of 135 TOC content measurements, 141 Rock-Eval pyrolysis analyses and 27 vitrinite reflectance measurements were used to evaluate the regional distribution and depth trends for the entire Carpathian Foredeep. The thermal maturity of organic matter is between the immature part and peak of the oil window (T_{max} = 413–448°C). Beneath the Western Carpathian Thrust Belt, the thermal maturity reaches higher values (R_r = 0.43–0.58%, T_{max} = 429–448°C). The hydrocarbon generation potential is poor or fair, even if the total organic carbon values indicate good or even very good source rock potential. This is mainly due to the prevailing gas-prone Type III kerogen. The best source rocks were observed in the Miocene strata of the southern and central segments of the area discussed.

Key words: Carpathian Foredeep, Miocene, organic petrography, thermal maturity, kerogen type, source rock potential

INTRODUCTION

The origin of organic matter-rich sediments depends on specific sedimentary conditions, such as high biological production, a low-energy sedimentary environment, a slow sedimentation rate and an absence of decomposition/oxidation processes (Pedersen and Calvert, 1990; Killops and Killops, 2005; Jovančićević and Schwarzbauer, 2015). A sufficient amount of organic matter, expressed as total organic carbon content (TOC), is one of the three parameters that indicate whether a rock will be a good source rock. Other parameters required to evaluate the source rock potential are the quality/type of organic matter and thermal maturity (Tissot and Welte, 1984). At least 0.5 wt.% of total organic carbon content is necessary for a rock unit to be considered as a source rock. Source rocks containing TOC in the range 0.5–2.0 wt.% are classified as satisfactory (fair, good), those with TOC >2 wt.% are considered as very good, and TOC values >4 wt.% characterize excellent source rocks (Peters and Cassa, 1994).

* Corresponding author, e-mail: gerslova@mail.muni.cz

Received: April 27, 2021; accepted: November 30, 2021; first published online: April 26, 2022

The genetic type of organic matter can be determined by the elemental analysis of kerogen (concentrations of C, H, O, N and S; Tissot and Welte, 1984). As this analytical approach requires time-consuming separation of kerogen, a routinely applied method for kerogen type identification uses hydrogen index (HI) and oxygen index (OI) from Rock-Eval pyrolysis (e.g., Espitalié et al., 1985a; Lafargue et al., 1998; Behar et al., 2001; Dahl et al., 2004).

Organic petrology analysis is considered as a complementary method to Rock-Eval analysis, especially if a mixed type of kerogen was identified (e.g., type II–III). Organic matter in sedimentary rocks is described as macerals that represent original biological material. Macerals are divided into three groups – huminite/vitrinite, liptinite, and inertinite. The difference between huminites and vitrinites is in how they transform humic constituents with increasing degrees of coalification (Taylor et al., 1998; Suárez-Ruiz et al., 2006). The H/C and O/C atomic ratios as well as HI and OI indices decrease with increasing rank within the huminite/vitrinite group (Espitalié et al., 1985a; Sýkorová et al., 2005). The liptinite group is high in hydrogen and its macerals are derived from plant spores, cuticles, resins, and algal bodies not necessarily related to the marine environment (Pickel et al., 2017). The inertinite group is typified by low hydrogen and high oxygen and carbon contents and represents kerogen type IV, which is oxidized organic matter, charcoal, or recycled organic matter (ICCP, 2001).

The increasing burial temperature results in changes in the optical and chemical properties of organic matter, which are

measurable in rock samples (Allen and Allen, 2013). Progressive changes are related to kinetic processes, in addition to temperature, and also depend on the time of exposure of organic matter to a given temperature (e.g., Littke et al., 2008; Hantschel and Kauerauf, 2009). Thermal maturity data sourced from deep boreholes are effective tools for palaeogeothermal gradient evaluation. The basin thermal history has an important controlling effect on the generation and distribution of hydrocarbons. Thermal maturity indicates diagenetic changes of organic matter dispersed in the source rocks that generate hydrocarbons – from the immature stage through the main phase of oil and gas production to the post-maturity stage.

A comprehensive overview of hydrocarbon systems for the Carpathian belt and its foreland along the southeastern margin of the Bohemian Massif, which includes the generation, migration, accumulation, and preservation of hydrocarbons, was provided by Picha et al. (2006). The potential source rocks investigated to date are primarily the Upper Jurassic and Lower Oligocene, and to a lesser degree also the Middle Devonian and Upper Carboniferous, successions (Krejčí et al., 1994, 1996; Geršlová et al., 2015; Jirman et al., 2019; Opletal et al., 2019). Miocene strata have not been considered as potential source rocks in these studies. However, extensive research into organic matter and its potential in the Polish and Ukrainian parts of the Carpathian Foredeep have demonstrated that the Miocene sedimentary rocks contain mostly gas-prone Type III kerogen and can also generate biogenic gas (Kotarba and Koltun, 2006; Kotarba et al., 2011a, b; Kosakowski et al., 2020). Moreover, burial modelling and gas geochemical analyses of the Carpathian Foredeep source rocks in Poland (Kotarba and Koltun, 2011; Kosakowski et al., 2020) and the Czech Republic (Goldbach et al., 2017) indicated local potential for generation of thermogenic gas. However, no systematic study of the thermal maturation has been conducted on the Miocene sedimentary rocks of the Carpathian Foredeep in the territory of the Czech Republic. This paper fills this gap and comprehensively describes the thermal maturity of these Miocene rocks, and defines the source rock properties and their relations to the current tectonic position of the Miocene strata in this area.

GEOLOGICAL SETTING

The Miocene deposits studied belong to the Moravian part of the Western Carpathian Foredeep – a peripheral foreland basin formed through the tectonic emplacement and crustal loading of the Western Carpathian Thrust Front onto the passive margin of the Bohemian Massif (Nehyba and Šikula, 2007; Fig. 1). The Western Carpathian Foredeep continues into the Polish Carpathian Foredeep Basin north-eastwards (Oszczypko et al., 2006) and to the North Alpine-Foreland Basin (Austrian Molasse Basin/Alpine Molasse Zone) to the south-west. To the east/south-east, the foredeep succession is overridden by the Western Carpathian Thrust Belt tectonic units. Overthrusting of at least 30 km was demonstrated by deep boreholes (Stráník et al., 1993; Eliáš and Pálenský, 1998; Oszczypko et al., 2006).

Local and regional unconformities within the Miocene succession are developed due to the varying intensity and orientation of flexural loading and different inherited geological and tectonic basement structure, as well as due to the polyphase nature of the active basin margin and a gradual change in its position (Brzobohatý and Cicha, 1993; Eliáš and Pálenský, 1998; Nehyba and Petrová, 2000; Krzywiec, 2001; Kováč et al., 2003, 2004; Oszczypko et al., 2006; Nehyba and Šikula, 2007; Francírek and Nehyba, 2016).

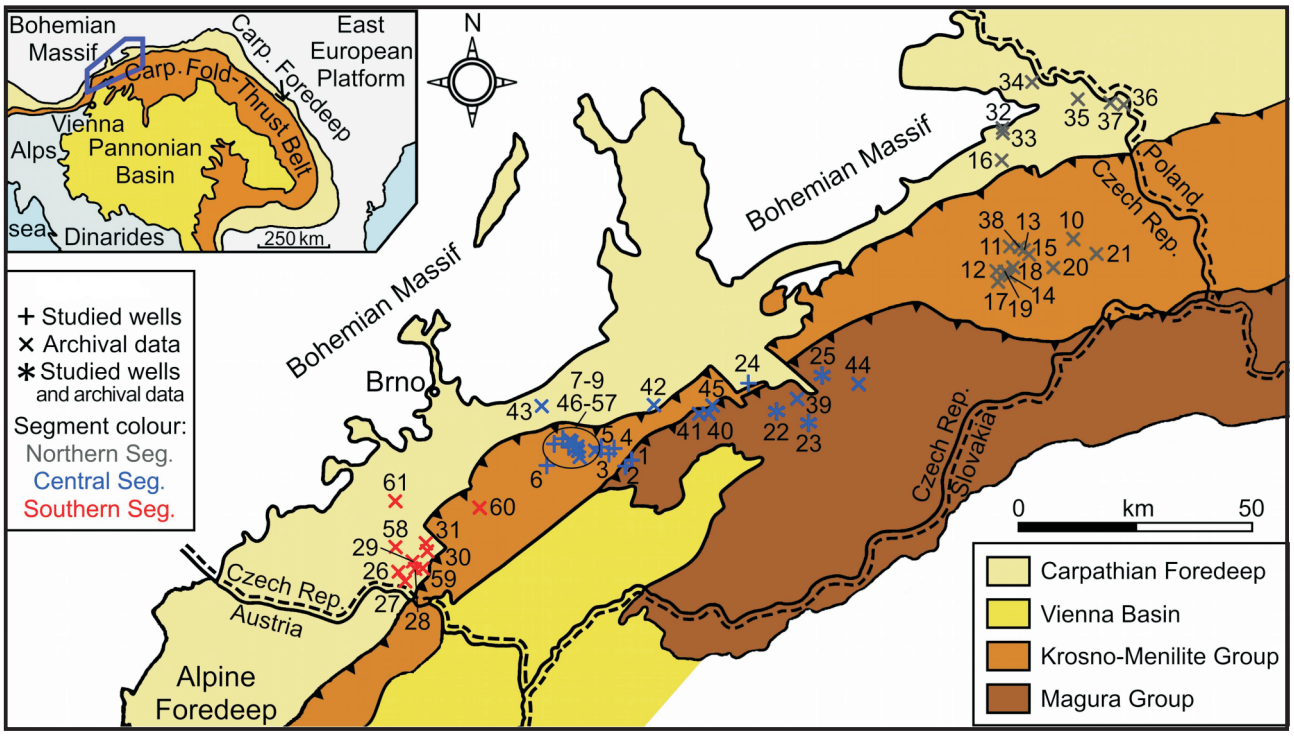

Fig. 1. Schematic geological map (modified after Pícha et al., 2006) with location of the boreholes studied

For borehole numbering see Appendices 1 and 2

Seismic and borehole data show that the bedrock in the area studied consists of Proterozoic crystalline rocks of Brunovistulicum, Devonian to Lower Carboniferous carbonates, and Carboniferous siliciclastic deposits – "Culm facies" of the Moravian-Silesian Paleozoic (Jirman et al., 2018). Erosional relics of Jurassic and autochthonous Paleogene strata are also present, especially in the southern segment of the area analysed (Fig. 1) where the Miocene depositional system overlies the Nesvačilka and Vranovice palaeovalleys (Kalvoda et al., 2003, 2008; Zágoršek et al., 2012; Hladilová et al., 2014). The basement generally dips south-eastwards; however, the relief is very irregular. In the S and SE part of the basin the basement is mostly overlain by Lower Miocene deposits, whereas the Middle Miocene cover is more completely developed towards the N and NW.

The Karpatian Stage sedimentary strata constitute the major part of the basin infill. This is particularly true for the central segment of the basin, where Francírek and Nehyba (2016) identified three successive depositional units:

- I – lagoon-estuary and barred coastline deposits,
- II – coastline to shallow marine deposits,
- III – offshore deposits.

The succession of depositional units reflects both a stepwise migration of the foredeep basin axis and a shift in time of the basin depocentre cratonwards. This, together with the forebulge retreat, attests to a shift of the basin axis to the north-west due to continued thrusting of the Outer Carpathian Flysch Wedge (Brzobohatý and Cicha, 1993).

The Karpatian deposits are lithostratigraphically subdivided into the Laa Formation (Mušov and Nový Přerov members) and the overlying Kroměříž Formation (Fig. 2). The Mušov Member is represented by grey marine mudstones rich in microfauna ("Schlier"). The Nový Přerov Member is formed of siltstones and mudstones with thin interbeds of fine- to medium-grained sandstone ("Sandy Schlier Formation") (Brzobohatý and Cicha, 1993; Adámek et al., 2003). Highly variable and even chaotic deposits of the Kroměříž Formation represent the final pulse of the Karpatian Stage depositional cycle (Benada and Kokolusová, 1986; Adámek et al., 2003).

Continuation of thrusting of the Outer Carpathian Flysch wedge by the end of the Karpatian led to the overriding of a significant part of the Carpathian Foredeep by flysch nappes, and partial incorporation of the basin deposits into the nappe structures. In the Polish Carpathian Foredeep, the part located beneath the Carpathian nappes has been defined as the inner foredeep (Waśkowska et al., 2014).

METHODOLOGY AND DATA

The Moravian part of the Carpathian Foredeep is subdivided in this study into three segments (southern, central, and northern). Each segment reveals partly different lithological content, stratigraphic range, depositional history, and basin architecture. The results presented are based on evaluation of data newly acquired from the central segment and archival data from the southern and northern segments. In total, 25 core samples from 13 boreholes were selected for maceral analyses and huminite reflectance. Analytical data obtained in the past, but never published, are also used in this work. These are the results of 135 analyses of TOC, 141 Rock-Eval pyrolysis analyses from 39 boreholes (Fig. 1 and Appendix 1), and 27 vitrinite reflectance analyses from 18 boreholes (Fig. 1 and Appendix 2).

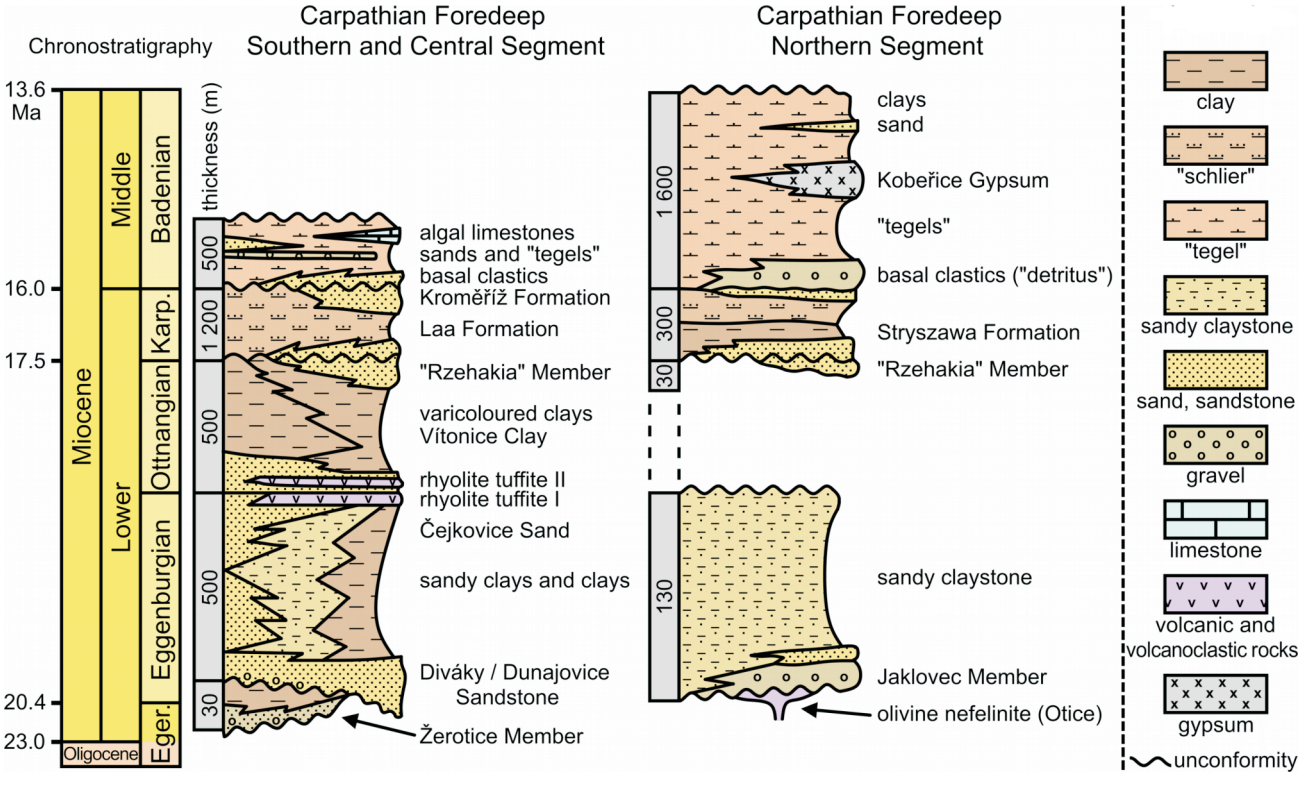

Fig. 2. Stratigraphy of the Neogene Foredeep in Moravia (modified after Adámek, 2003; Nehyba et al., 2019a, b)

The huminite/vitrinite reflectance and maceral evaluation was carried out by *Olympus BX51* microscope with a *Zeiss Photomultiplier MK3* system, an immersion lens with 40x magnification, and Pelcon point counter. OLYMPUS Immersion Oil Type-F was used. Random reflectance was determined on polished sections by *SpectraVision* software calibrated with spinel (R = 0.422%), sapphire (R = 0.596%), and yttrium aluminium garnet (R = 0.894%). Between 50 and 100 points were evaluated on each sample.

Total organic carbon (TOC, wt.%) was measured using pulverised samples after decarbonatization with concentrated phosphoric acid. The quantity of the carbon dioxide released during burning of the sample at 900°C was subsequently measured with an IR detector. The Rock-Eval data were received using a Rock-Eval II apparatus applying cycle 1 (Espitalié et al., 1985b). They are: the free hydrocarbons content S_1 (mg HC/g rock) evaporated from the sample at 300°C, residual hydrocarbons (or residual hydrocarbon potential) S_2 (mg HC/g rock) released in the temperature range from 300 to 600°C, and temperature T_{max} (°C) at the S_2 peak maximum. The genetic potential (GP) represents the sum of both the S_1 and S_2 peaks (mg HC/g rock) and the production index was calculated using the formula PI = $S_1/(S_1+S_2)$ (Espitalié et al., 1985b). The hydrogen index (HI) was calculated using the previously determined TOCas HI = 100 S_2/TOC (mg HC/g TOC).

RESULTS

TOC CONTENT AND ROCK-EVAL DATA

The detailed results of the Rock-Eval analyses are given in Appendix 1. Whereas the average TOC is similar in both the central and southern segments (1.35 and 1.36 wt.% respectively), it is markedly lower in the northern segment (0.99 wt.%, Table 1). The highest average GP of 3.4 mg HC/g rock calculated on the samples from the southern segment decreases to 2.8 mg HC/g rock in the central segment. In the northern segment samples, a GP of only 0.55 mg HC/g rock was calculated. The average HI reaches 182 mg HC/g TOC in the southern segment, 174 mg HC/g TOC in the central segment and only 54 mg HC/g TOC in the northern segment (Table 1). The average T_{max} is similar in the central and northern segment samples (432 and 431°C, Fig. 3) and slightly lower in the samples from the southern segment (426°C).

RANDOM HUMINITE/VITRINITE REFLECTANCE

In the southern segment, the huminite reflectance ranges from 0.27 to 0.43% R_r with a standard deviation of 0.03–0.08% (Fig. 4, Table 2 and Appendix 2). These values represent a 500 m thick interval from 801 to 1296 m depth and devoid of any visible vertical trend. The rock maturity corresponds to the immature zone and/or lignite to sub-bituminous coal. In the central segment, the random huminite/vitrinite reflectance varies in a wider range from 0.22 to 0.58% R_r with a standard deviation of 0.03–0.10 (Fig. 4, Table 2 and Appendix 2). The organic matter reaches up to the boundary between the immature and mature stage that is equal to lignite up to the upper margin of sub-bituminous coal. The samples analysed cover a wide depth interval from 765 to 4729 m.

The random reflectance values show considerable variations but no increasing trend within the depth range 0–2 km despite a gradual increase in thermal maturity with depth (Fig. 4).

Huminite/vitrinite reflectance ranges from 0.34 to 0.58% R_r in the northern segment (Fig. 4 and Appendix 2). In borehole NP-779 (ID 16 in Fig. 1), situated ahead of the West Carpathian orogenic front, maturity reaches 0.36% R_r at a depth of 179 m. However, the strata intersected beneath the Carpathian nappes at a depth of 887 m in borehole Lhotka-5 (ID 13 in Fig. 1) show a comparable reflectivity (0.34% R_r). This similarity suggests that the observed maturity level was reached before the Carpathian nappes overrode the Miocene succession of the Foredeep.

ORGANIC PETROGRAPHY

The results of qualitative and quantitative analyses of the maceral composition in the Miocene samples of the central segment are listed in Table 2. A huminite maceral group composed predominantly of ulminite and attrinite is present mostly in samples from Tlumačov-1, Lukov-1, Koryčany-9, and 13, Mouchnice-1 and 2, Snovídky-1, Žarošice-2, Ždánice-135, 147 and 175 boreholes (Table 2).

A higher range of vitrinite reflectance, from 0.44 to 0.58% R_r, was measured in the Gottwaldov-1 and 2 boreholes where the Miocene rocks are deeply buried beneath the West Carpathians. The vitrinite maceral group, composed predominantly of collotelinite and vitrodetrinite, is present in samples from the Gottwaldov-1 and 2 boreholes (Table 2). The liptinite maceral group is composed mainly of alginite that is observed as thin-

Table 1

TOC and Rock-Eval proxies of Miocene sedimentary rocks in individual segments of the Carpathian Foredeep in Moravia (based on data from Appendix 1)

Parameter/ segment	TOC [wt.%]	S_1	S_2	GP	HI [mg HC/g TOC]	T_{max} [°C]	PI
		[mg HC/g rock]					
Northern	0.24–1.89 0.99	0.00–0.46 0.03	0.32–0.76 0.50	0.33–1.08 0.55	19–200 54	422–433 431	0.00–0.68 0.06
Central	0.12–9.17 1.36	0.01–4.15 0.39	0.04–17.7 2.45	0.06–21.1 2.84	3–506 174	413–448 432	0.01–0.96 0.15
Southern	0.53–2.90 1.35	0.01–0.76 0.25	0.23–8.55 3.20	0.24–8.65 3.44	44–434 182	419–431 426	0.01–0.14 0.06

TOC – total organic carbon, S_1 – free hydrocarbons content, S_2 – residual hydrocarbon potential, GP – genetic potential (GP = S_1 + S_2), HI – hydrogen index, T_{max} – temperature of maximum of S_2 peak, PI – production index; range of selected parameters is given as numerator, average values in denominator

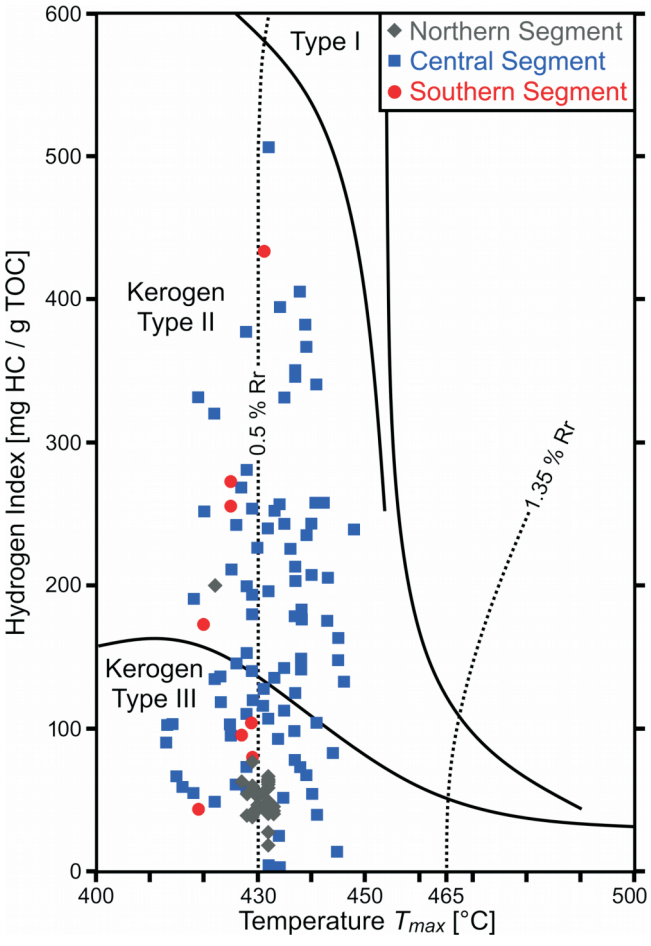

Fig. 3. The cross-plot of hydrogen index *versus* Rock-Eval temperature T_{max} classified the kerogen type and thermal maturity in the southern, central and northern segments of the Carpathian Foredeep

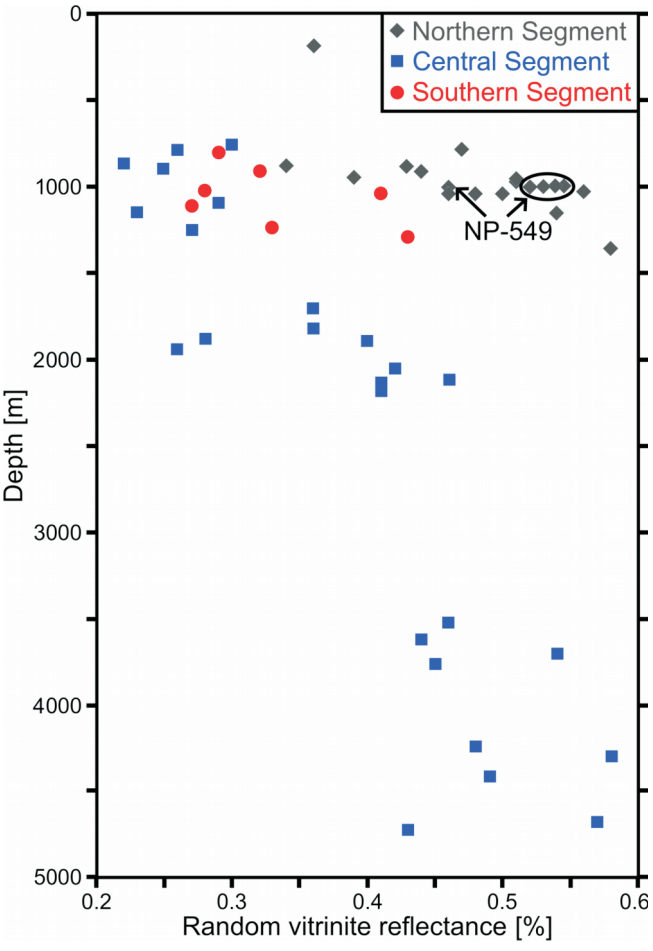

Fig. 4. Random vitrinite reflectance depth trends in the southern, central and northern segments of the Carpathian Foredeep

walled algae, either with or without pyrite infills. Liptodetrinite occurs as fine detritus disseminated in the rock. Other macerals such as sporinite, resinite, bituminite and cutinite are rare, or almost absent, and may not be found in all samples. The least represented group of macerals is inertinite (Table 2) composed of fuzinite. Alginite, ulminite, and collotelinite are commonly associated with pyrite, which occurs in all samples as framboidal crystal aggregates or single crystals.

Samples from the Ždánice-135, 147 and 175 boreholes (Fig. 5 and Table 2) are rich in organic matter that occurs in fine-grained silty mudstones with an occasional admixture of quartz sand grains. The most prominent components are ulminite and textinite of the huminite group, the particle size of which exceeds 100 μm. Organic particles appear to be homogeneous but also granular, porous and oxidized, and with a mineral admixture. Occasionally macerals are broken and/or stretched (Fig. 5A, A'). Liptinite occurs in the form of huminite infills, e.g., resinite (Fig. 5B, B') or separately dispersed in the mineral phase, e.g., alginite, sporinite and liptodetrinite. Inertinite occurs sporadically with the highest amount found in sample Ždánice-175 (Fig. 5D, D').

Samples from Koryčany-9 and 13, Mouchnice-1 and 2, Snovídky-1, and Žarošice-2 boreholes are fine-grained (silty mudstones) with occasional admixture of quartz sand grains. The most prominent maceral group is huminite, but its particles are predominantly small. The organic particles are mostly non-homogeneous, altered, granular, porous, and weathered. Liptinite occurs separately or as huminite infills. Rock samples collected from the Lukov-1 and Tlumačov-1 boreholes are fine-grained, poor in organic matter dominated by huminite macerals (Table 2), and rich in pyrite.

DISCUSSION

THERMAL MATURITY

Based on the average T_{max} and PI of Rock-Eval pyrolysis (432°C and 0.15, respectively), the strata of the central segment are entering the oil window (Figs. 3 and 6). The T_{max} and PI within both the northern segment (431°C and 0.06, respectively) and the southern segment (426°C and 0.06, respectively) indicate that deposits are thermally immature or at the initial stage of generation of the hydrocarbons, which is also supported by low reflectance values in the range 0.27–0.58% R_r. A higher range of vitrinite reflectance, from 0.44 to 0.58% R_r, was measured in the central segment in the Gottwaldov-1 and 2 boreholes where the Miocene rocks are deeply buried beneath the West Carpathians.

Variations in the thermal maturity of the sedimentary rocks within the southern segment are influenced by both burial depth

Table 2

The huminite/vitrinite random reflectance (R_r %) and petrographic composition of Miocene strata from the central segment of the Carpathian Foredeep

Borehole ID	Borehole	Depth [m]	R_r [%]	s [%]	V [%]	H [%]	L [%]	I [%]	M [%]
1	Koryčany-13	1879	0.28	0.07	–	0.9	0.0	0.0	99.1
2	Koryčany-9	1946	0.26	0.06	–	2.3	1.9	0.6	95.2
3	Mouchnice-1	1101	0.29	0.04	–	5.2	0.4	0.6	93.8
4	Mouchnice-2	1253	0.27	0.05	–	3.1	4.1	0.0	92.8
5	Snovídky-1	893	0.25	0.08	–	4.5	1.0	0.0	94.5
6	Žarošice-2	1152	0.23	0.06	–	4.3	0.2	0.0	95.5
7	Ždánice-135	787	0.26	0.07	–	6.6	2.7	0.0	90.7
8	Ždánice-147	866	0.22	0.05	–	9.4	5,7	0.0	84.9
9	Ždánice-175	765	0.30	0.03	–	22.2	3.1	1.0	73.7
22	Gottwaldov-1	3529	0.46	0.08	1.6	–	0.8	0.0	97.6
22	Gottwaldov-1	3625	0.44	0.07	0.4	–	1.0	0.2	98.5
22	Gottwaldov-1	3709	0.64	0.10	1.7	–	1.0	0.5	96.7
22	Gottwaldov-1	3768	0.45	0.09	1.6	–	1.6	0.2	96.5
23	Gottwaldov-2	4242	0.48	0.06	0.4	–	0.8	0.0	98.8
23	Gottwaldov-2	4300	0.49	0.07	2.0	–	4.2	0.0	93.8
23	Gottwaldov-2	4416	0.49	0.07	0.8	–	2.3	0.2	96.7
23	Gottwaldov-2	4682	0.57	0.12	1.4	–	1.2	0.2	97.2
23	Gottwaldov-2	4729	0.43	0.13	2.9	–	3.9	0.0	93.2
24	Tlumačov-1	1708	0.36	0.05	–	3.4	3.5	0.0	93.1
24	Tlumačov-1	1819	0.36	0.05	–	2.3	1.0	0.0	96.7
24	Tlumačov-1	1895	0.40	0.08	–	1.3	0.2	0.0	98.5
24	Tlumačov-1	2056	0.42	0.08	–	1.3	1.1	0.2	97.4
24	Tlumačov-1	2145	0.41	0.04	–	2.2	0.6	0.8	96.3
25	Lukov-1	2121	0.46	0.08	–	1.1	0.4	0.0	98.5
25	Lukov-1	2179	0.41	0.07	–	1.6	1.0	0.0	97.4

R_r – random reflectance of huminite/vitrinite, s – standard deviation, V – vitrinite maceral group content, H – huminite maceral group content, L – liptinite maceral group content, I – inertinite maceral group content, M – mineral matter content

and position within the basin. Samples closer to the eastern margin (i.e. orogenward) show relatively higher thermal maturity compared to the samples from the opposite side (i.e. cratonward margin). This situation is well illustrated by borehole Mikulov-4, located just in front of the thrust belt. Namely, the samples from the upper part of the sedimentary succession intersected (the Karpatian Stage) reveal T_{max} values similar to those of the samples from the deeper part (Eggenburgian to Karpatian). The interpreted 2D seismic line 289/83 (Fig. 7) demonstrates that the lower part of the sedimentary succession penetrated by the Mikulov-4 borehole (Mik-4) is deformed by compression exerted by the advancing Western Carpathian nappes. The relatively higher maturity of organic matter in the upper part of the Miocene strata can be explained by the fact that they were affected by increased tectonic stress near the thrust front.

All samples from the northern segment were exposed to tectonic stress. This can be seen in Figure 6 where thin slices of immature or low maturity strata are stacked and T_{max} does not gradually increase with depth. This relation is clearly illustrated by borehole NP-895 in which no vertical increase of T_{max} with depth (Fig. 6) is observed, or by a considerable variation of values over a short depth interval in NP-549 (Fig. 4). Such a maturity profile with depth indicates tectonic control related to the late phases of the Carpathian orogeny.

The same T_{max} range was observed among the results from the Polish and Ukrainian parts of the Carpathian Foredeep. The low thermal maturity expressed as T_{max} varying between 427–430°C was measured in the Lower Badenian–Lower Sarmatian rocks in the Ukrainian Carpathian Foredeep Basin (Kotarba et al., 2011b) and T_{max} in the range 419–438°C was recorded in the Upper Badenian–Lower Sarmatian sedimentary rocks in Poland (Czepiec and Kotarba, 1998).

Published research (Kosakowski et al., 2020) indicates that in the outer part of the Carpathian Foredeep in Poland, the minimum burial depth required to reach R_r = 0.5% is 3000 m. Such burial depths occur in Poland only there where the Middle Miocene strata are buried beneath the Carpathian overthrust. In the Czech Republic, the Middle Miocene deposits are buried beneath the Carpathian nappes to depths of ~4000 m within the central segment and show increased thermal maturity with a slight shift towards thermogenic hydrocarbon generation.

A comprehensive assessment of hydrocarbons over a wider area demonstrates the key role of the Carpathian overthrust regardless of the age of the potential source rock. The investigation of the Miocene strata in Poland and Ukraine reveals that thermogenic HC generation begins below the depth of 2500 m (Kotarba et al., 2011a; Kosakowski and Wróbel, 2012; Pupp et al., 2018). Detailed studies suggest that the hydrocarbons were not expelled from all potential source rocks (Pícha et al., 2006; Buzek et al., 2019), and the best conditions for hydrocarbon generation occurred in areas deeply buried under the Outer Western Carpathian units and thus these can still be active.

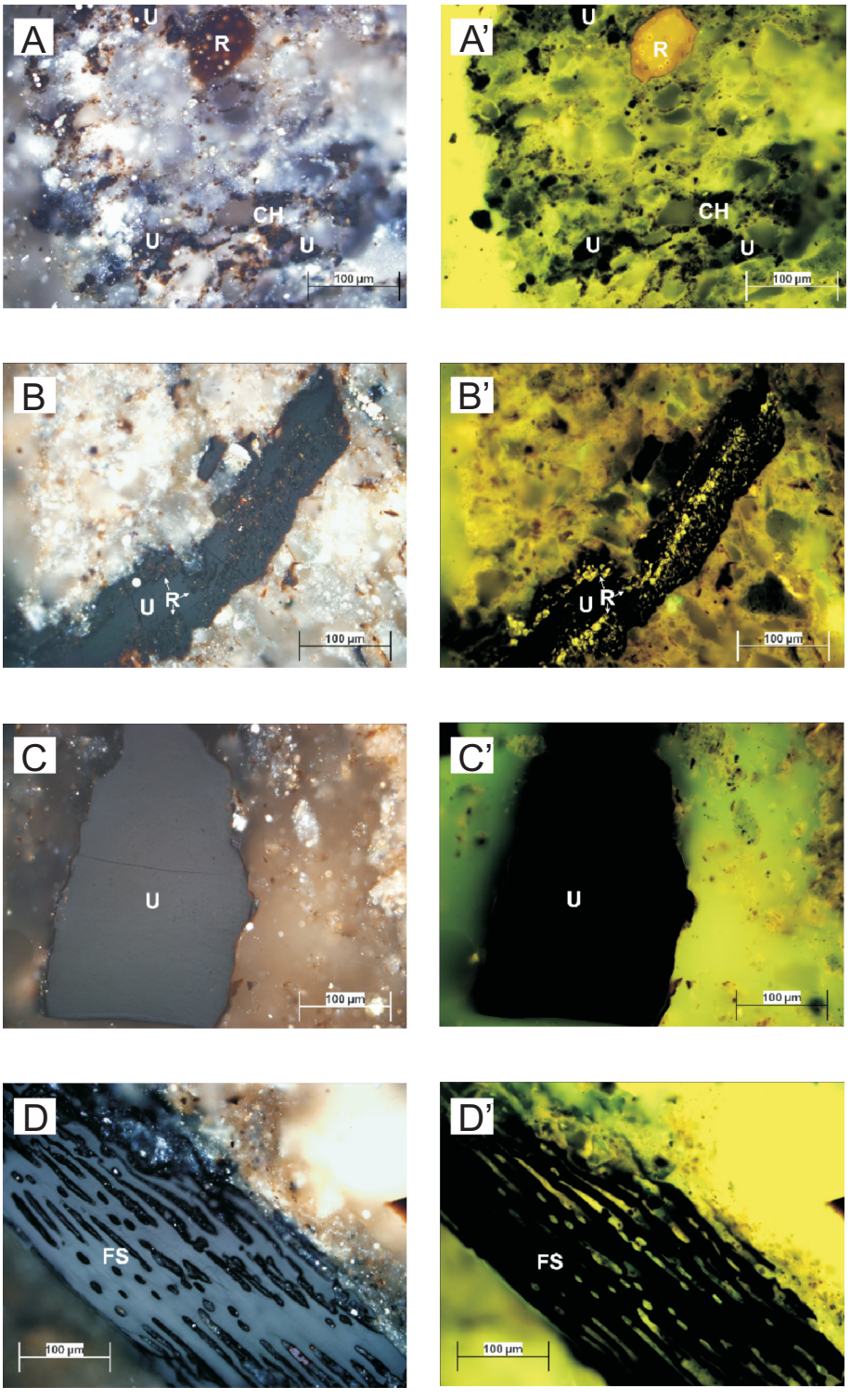

Fig. 5. Photomicrographs of dispersed organic matter in the Miocene strata

A, A' – rounded, partially weathered resinite (R) with yellowish-brownish fluorescence (A') and fragments of ulminite (U) and corpohuminite (CH) in the coarse-grained mineral fraction – borehole Ždánice-135 (787 m); **B, B'** – ulminite (U) with the transition to textinite filled with resinite (R); borehole Ždánice-147 (866 m); **C, C'** – ulminite (U); borehole Ždánice-175 (765 m); **D, D'** – fusinite (FS) with conserved cellular structure; borehole Ždánice-175 (765 m)

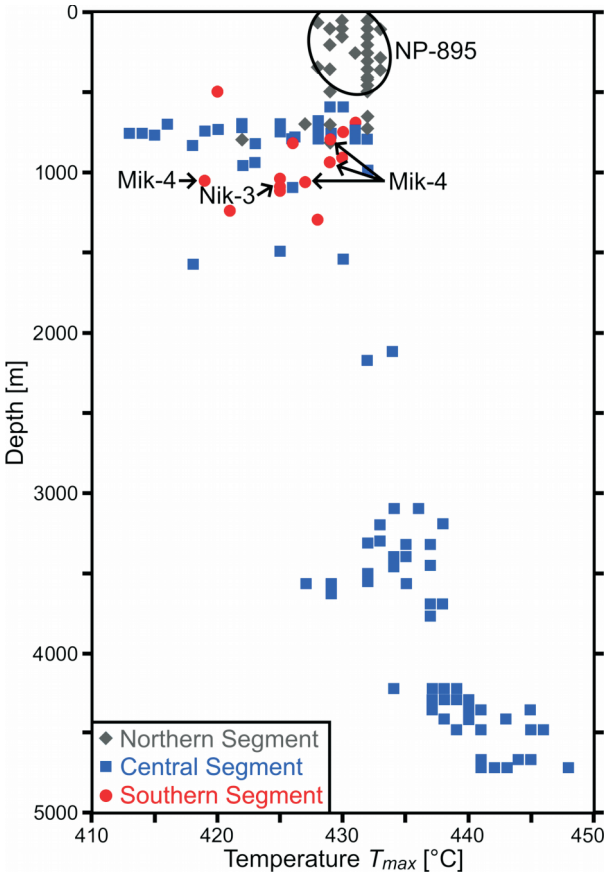

Fig. 6. The Rock-Eval T_{max} depth trends in the southern, central and northern segments of the Carpathian Foredeep

The high range of values in a relatively small depth interval demonstrates that the rearrangement of the Miocene succession caused by the overthrusting of the West Carpathian nappe system deformed the stratigraphic sequence so much that it is not possible to reconstruct a reliable geothermal gradient based on available data.

KEROGEN TYPE

The kerogen type is commonly inicated by the diagram of HI *versus* temperature T_{max}. This cross-plot indicates prevailing kerogen types II and III within both the southern (HI up to 434 mg HC/g TOC) and central segments (HI up to 506 mg HC/g TOC; Fig. 3). Significantly, lower HI values, of 54 mg HC/g TOC on average, which are typical of kerogen type III, were observed within the northern segment samples (Appendix 1). However, the kerogen type interpretations based on the Rock-Eval data may be influenced by low TOC (<0.5–1.0 wt.%) in the samples causing the underestimation of true HI (Peters and Cassa, 1994; Dahl et al., 2004) and the mineral-matrix effect (Więcław, 2016).

Within the southern segment, the predominant macerals are represented mostly by huminite pointing to their terrestrial origin. This corresponds well to the low HI and classifies the organic matter as type III kerogen.

However, liptinite macerals composed mainly of spores and pollen were observed in larger amounts within the Miocene strata in the Gottwaldov-1 and -2 boreholes (central segment, Table 2). This observation is in agreement with the higher HI values (Fig. 3). The increase in HI is caused by a relatively higher content of liptinite macerals, which is interpreted as reflecting the presence of distal marine facies within the Carpathian Foredeep. Significant variations in depositional environments are documented in the successions from which samples representing the central

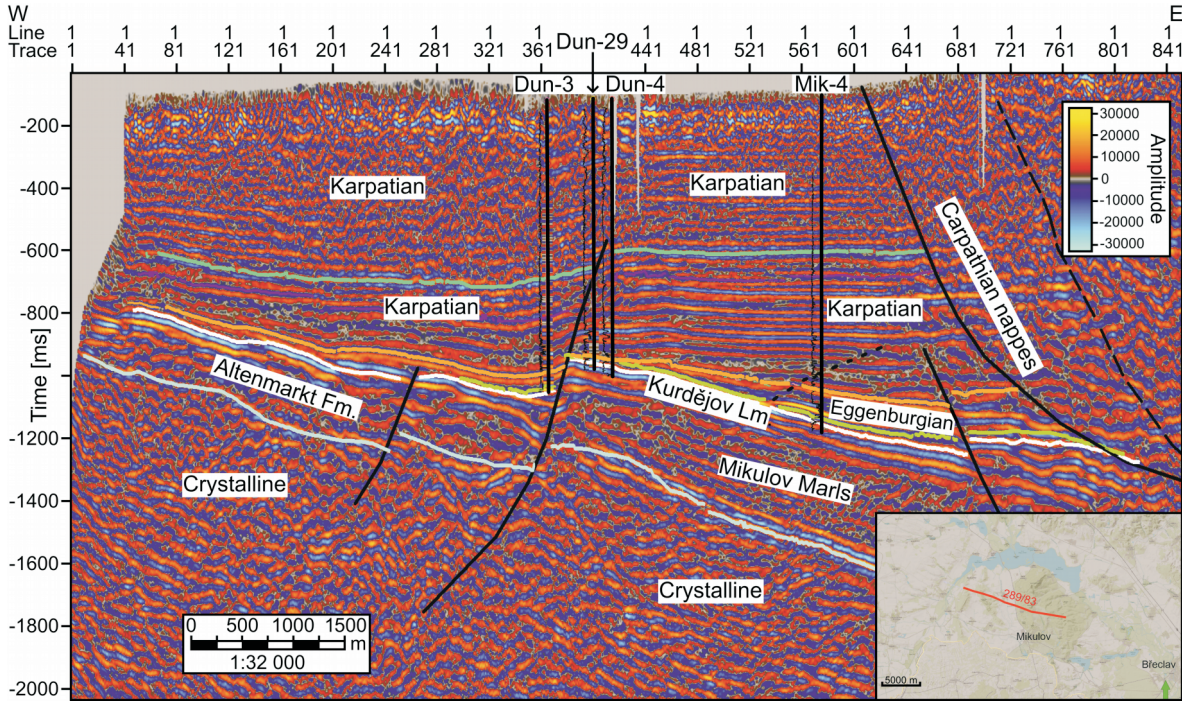

Fig. 7. Geological interpretation of the 2D seismic line 289/83 across the southern segment of the Carpathian Foredeep in the Czech Republic

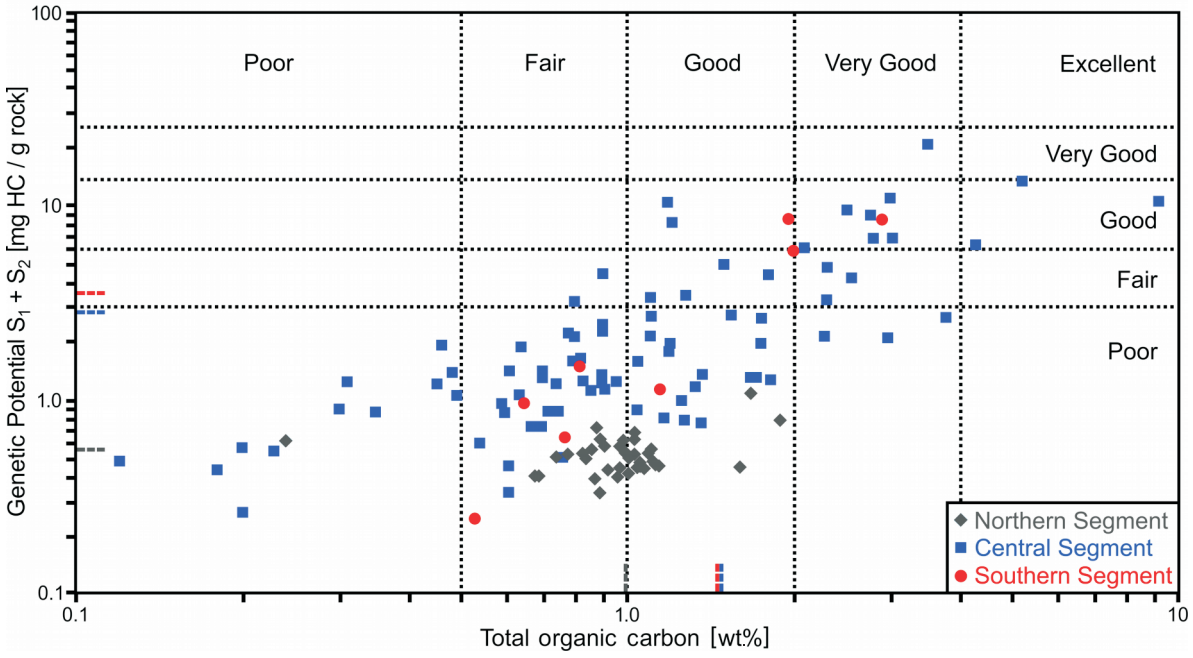

Fig. 8. Source rock potential of the Miocene samples

Criteria according to Peters and Cassa (1994); average values for individual segments marked by coloured dashed line

segment are derived. The following depositional settings were interpreted here by Francírek and Nehyba (2016): alluvial and fluvial, brackish lagoon-estuary, clastic coast (foreshore, shore-face), nearshore (shore-face/transitional zone to inner shelf), shallow marine (inner and outer shelf). Thus, deposits of very diverse environments occur in a restricted area, and such a palaeogeographic scenario does not promote the formation of promising source rocks.

SOURCE ROCK POTENTIAL

The source rock potential of samples from the northern, central, and southern segments (Fig. 8) was evaluated based on the cross-plot of GP (Rock-Eval $S_1 + S_2$) *versus* TOC according to Peters and Cassa (1994). The best source rock potential was observed in the Miocene samples from the southern and central segments. However, based on the GP, even here samples with "poor to fair" potential prevail over the ones with "good" potential, even if the TOC indicates "good" to "very good" potential (Fig. 8). This discrepancy may be explained by the presence of the less prolific gas-prone Type III kerogen generating small amounts of hydrocarbons. The studies of Baskin (1997) provided evidence that only ~10% of the initial TOC content may be converted into hydrocarbons during full maturation of the Type III kerogen. The data from the northern segment indicate "poor" source rock quality based on the GP, even if the TOC indicates "fair to good" potential.

CONCLUSIONS

Based on the Rock-Eval temperature T_{max} (413–448°C) and vitrinite/huminite reflectance (0.2–0.6% R_r), the thermal maturity of organic matter in the Carpathian Foredeep in the Czech Republic ranges between the immature and initial stage of hydrocarbon generation. Thermal maturity indicators, vitrinite reflectance and pyrolysis T_{max} reach higher values below the Western Carpathian Thrust Belt in the Gottwaldov-1 and -2 boreholes in the central segment. A higher maturity in the northern segment is observed in the tectonically modified section where no increase of T_{max} or R_r with depth was documented. The source rock potential is poor to fair based on the genetic potential (Rock-Eval $S_1 + S_2$), even where the TOC concentration may be evaluated as showing good to very good potential. The best source rock potential was observed in the Miocene samples from the southern and central segments where the organic matter is Type III, gas-prone kerogen.

Acknowledgements. This work was carried out thanks to the institutional support of Masaryk University in Brno. It could not have been completed without samples, archival data and seismic profiles kindly provided by MND a.s., Úprkova 807/6, 695 01 Hodonín, Czech Republic. We also thank an anonymous reviewer and Y. Koltun for their remarks and comments, which significantly improved the quality of the manuscript.

REFERENCES

Adámek, J., 2003. The Miocene of the Carpathian Foredeep in southern Moravia, geological development and lithostratigraphic classification (in Czech with English summary). Geoscience Research Reports: 9–11.

Adámek, J., Brzobohatý, R., Pálenský, P., Šikula, J., 2003. The Karpatian in the Carpathian foredeep (Moravia). In: The Karpatian, a lower Miocene stage of the central Paratethys (eds. R. Brzobohatý, I. Cicha, M. Kováč and F. Rögl): 75–88. Masaryk University, Brno.

Allen, P.A., Allen, J.R., 2013. Basin Analysis: Principles and Applications. Blackwell Publishing.

Behar, F.V., Beaumont, B. de, Penteado H.L., 2001. Rock-Eval 6 technology: performances and developments: Oil and Gas Science and Technology – Revue du l'Institute Français du Petrole, **56**: 111–134.

Baskin, D.K., 1997. Atomic H/C ratio of kerogen as an estimate of thermal maturity and organic matter conversion. AAPG Bulletin, **81**: 1437–1450.

Benada, S., Kokolusová, A., 1986. New findings on the geological position of clasts in the central part of the Carpathian foredeep in Moravia (in Czech with English summary). Zemní Plyn a Nafta, **32**: 1–15.

Brzobohatý, R., Cicha, I., 1993. Carpathian foredeep (in Czech with English summary). In: Geologie Moravy a Slezska (eds. A. Přichystal, V. Obstová and M. Suk): 123–128. Moravské Zemské Muzeum a Sekce Geologických věd Přírodovědecké Fakulty Masarykovy University, Brno.

Buzek, F., Geršlová, E., Geršl, M., Čejková, B., Jacková, I., Lneničková, Z., 2019. Evaluation of the gas content in archived shale samples: a carbon isotope study. Geosciences, **2019**, 9: 481.

Czepiec, I., Kotarba, M., 1998. Paleoecology and organic matter in the Late Badenian and Early Sarmatian marine basin of the Polish part of the Carpathian Foredeep. Przegląd Geologiczny, **46**: 732–736.

Dahl, B., Bojesen-Koefoed, J., Holm, A., Justwan, H., Rasmussen, E., Thomsen, E., 2004. A new approach to interpreting Rock-Eval S2 and TOC data for kerogen quality assessment. Organic Geochemistry, **35**: 1461–1477.

Eliáš, M., Pálenský, P., 1998. Model of the formation of Miocene foredeep in the Ostrava region (in Czech with English summary). Geoscience Research Reports: 65–66.

Espitalié, J., Deroo, G., Marquis, F., 1985a. La pyrolyse Rock-Eval et ses applications. Deuxieme partie. Revue du l'Institute Français du Pétrole, **40**: 755–784.

Espitalié, J., Deroo, G., Marquis, F., 1985b. La pyrolyse Rock-Eval et ses applications. Premiere partie. Revue du l'Institute Français du Pétrole, **40**: 563–579.

Francírek, M., Nehyba, S., 2016. Evolution of the passive margin of the peripheral foreland basin: An example from the Lower Miocene Carpathian Foredeep (Czech Republic). Geologica Carpathica, **67**: 41–68.

Geršlová, E., Opletal, V., Sýkorová, I., Sedláková, I., Geršl, M., 2015. A geochemical and petrographical characterization of organic matter in the Jurassic Mikulov Marls from the Czech Republic. International Journal of Coal Geology, **141–142**: 42–50.

Goldbach, M., Geršlová, E., Misz-Kennan, M., Nehyba, S., 2017. Thermal maturity of Miocene organic matter from the Carpathian Foredeep in the Czech Republic: 1D and 3D models. Marine and Petroleum Geology, **88**: 18–29.

Hantschel, T., Kauerauf, A., 2009. Fundamentals of Basin and Petroleum Systems Modeling. Springer, Berlin Heidelberg.

Hladilová, Š., Nehyba, S., Zágoršek, K., Tomanová Petrová, P., Bitner, M.A., Demeny, A., 2014. Early Badenian transgression on the outer flank of Western Carpathian Foredeep, Hluchov area, Czech Republic. Annales Societatis Geologorum Poloniae, **84**: 259–279.

International Committee for Coal and Organic Petrology, (ICCP), 2001. The new inertinite classification (ICCP System 1994). Fuel, **80**: 459–471.

Jirman, P., Geršlová, E., Kalvoda, J., Melichar, R., 2018. 2D basin modelling in the eastern Variscan fold belt (Czech Republic): influence of thrusting on patterns of thermal maturation. Journal of Petroleum Geology, **41**: 175–188.

Jirman, P., Geršlová, E., Bubík, M., Sachsenhofer, R.F., Bechtel, A., Więcław, D., 2019. Depositional environment and hydrocarbon potential of the Oligocene Menilite Formation in the Western Carpathians: a case study from the Loučka section (Czech Republic). Marine and Petroleum Geology, **107**: 334–350.

Jovančićević B., Schwarzbauer, J., 2015. Fossil Matter in the Geosphere. Springer International Publishing Switzerland.

Kalvoda, J., Leichmann, J., Bábek, O., Melichar, R., 2003. Brunovistulian Terrane (Central Europe) and Istanbul Zone (NW Turkey): Late Proterozoic and Paleozoic tectonostratigraphic development and paleogeography. Geologica Carpathica, **54**: 139–152.

Kalvoda, J., Bábek, O., Fatka, O., Leichmann, J., Melichar, R., Špaček, P., 2008. Brunovistulian terrane (Bohemian Massif, Central Europe): from late Proterozoic to late Paleozoic: a review. International Journal of Earth Sciences, **97**: 497–518.

Killops, S., Killops, V., 2005. Introduction to Organic Geochemistry. Blackwell, Oxford.

Kosakowski, P., Wróbel, M., 2012. Burial history, thermal history and hydrocarbon generation modelling of the Jurassic source rocks in the basement of the Polish Carpathian Foredeep and Outer Carpathians (SE Poland). Geologica Carpathica, **63**: 335–342.

Kosakowski, P., Machowski, G., Kowalski, A., Koltun, Y.V., Zakrzewski, A., Sowiżdżał, A., Stadtmuller, M., 2020. Organic geochemistry of middle Miocene (Badenian-Sarmatian) source rocks and maturation modelling in the Polish and Ukrainian sectors of the external Carpathian Foredeep. Journal of Petroleum Geology, **43**: 277–300.

Kotarba, M.J., Koltun, Y.V., 2006. Origin and habitat of hydrocarbons of the Polish and Ukrainian parts of the Carpathian Province. AAPG Memoir, **84**: 395–443.

Kotarba, M.J., Koltun, Y.V., 2011. Origin of natural gases in the autochthonous Miocene strata of the Ukrainian Carpathian Foredeep and its Mesozoic basement. Annales Societatis Geologorum Poloniae, **81**: 425–441.

Kotarba, M.J., Peryt, T.M., Koltun, Y.V., 2011a. Microbial gas system and prospectives of hydrocarbon exploration in Miocene strata of the Polish and Ukrainian Carpathian Foredeep. Annales Societatis Geologorum Poloniae, **81**: 523–548.

Kotarba, M.J., Więcław, D., Kosakowski, P., Koltun, Y.P., Kowalski, A., 2011b. Evaluation of hydrocarbon potential of the autochthonous Miocene strata in the NW part of the Ukrainian Carpathian Foredeep. Annales Societatis Geologorum Poloniae, **81**: 395–407.

Kováč, M., Andreyeva-Grigorovich, A.S., Brzobohatý, R., Fodor, L., Harzhauser, M., Oszczypko N., Pavelić, D., Rögl, F., Saftić, B., Sliva, S., Stráník, Z., 2003. Karpatian paleogeography, tectonics and eustatic changes. In: Karpatian – a Lower Miocene stage of the Central Paratethys (eds. R. Brzobohatý, I. Cicha, M. Kováč and F. Rögl): 49–72. Masaryk University, Brno.

Kováč, M., Baráth, I., Harzhauser, M., Hlavatý, I., Hudáčková, N., 2004. Miocene depositional systems and sequence stratigraphy of the Vienna basin. Courier Forschungsinstitut Senckenberg, **246**: 187–212.

Krejčí, O., Franců, J., Müller, P., Pereszlenyi, M., Straník, Z., 1994. Geologic structure and hydrocarbon generation in the Carpathian flysch belt of southern Moravia. Bulletin of the Czech Geological Survey, **69**: 13–26.

Krejčí, O., Franců, J., Poelchau, H.S., Müller, P., Stráník, Z., 1996. Tectonic evolution and oil and gas generation model in the

contact area of the North European Platform with the West Carpathians. EAGE Special Publication, **5**: 177–186.

Krzywiec, P., 2001. Contrasting tectonic and sedimentary history of the central and eastern parts of the Polish Carpathian foredeep basin – results of seismic data interpretation. Marine and Petroleum Geology, **18**: 13–38.

Lafargue, E., Marquis, F., Pillot, D., 1998. Rock-Eval 6 applications in hydrocarbon exploration, production, and soil contamination studies. Revue de l'Institut Français du Pétrole, **53**: 421–437.

Littke, R., Bayer, U., Gajewski, D., Nelskap, S., 2008. Dynamics of Complex Intracontinental Basins. Springer, Berlin Heidelberg.

Nehyba, S., Petrová, P., 2000. Karpatian sandy deposits in the southern part of the Carpathian Foredeep in Moravia. Bulletin of Czech Geological Survey, **75**: 53–66.

Nehyba, S., Šikula, J., 2007. Depositional architecture, sequence stratigraphy and geodynamic development of the Carpathian Foredeep (Czech Republic). Geologica Carpathica, **58**: 53–69.

Nehyba, S., Gilíková, H., Tomanová Petrová, P., Otava, J., Skácelová, Z., 2019a. Evolution of a sedimentary infill of a palaeovalley at a distal margin of the peripheral foreland basin. Geological Quarterly, **63** (2): 319–344.

Nehyba, S., Otava, J., Tomanová Petrová, P., Gazdová, A., 2019b. The foreland state at the onset of the flexurally induced transgression: data from provenance analysis at the peripheral Carpathian Foredeep (Czech Republic). Geologica Carpathica, **70**: 241–260.

Opletal, V., Geršlová, E., Nehyba, S., Sýkorová, I., Rez, J., 2019. Geology and thermal maturity of Namurian deposits in the Němčičky Sub-basin as the south-eastern continuation of the Upper Silesian Coal Basin (Czech Republic). International Journal of Coal Geology, **216**: 303–323.

Oszczypko, N., Uchman, A., Malata, E., 2006. Palaeotectonic Evolution of the Outer Carpathian and Pieniny Klippen Belt Basins (in Polish with English summary): 111–126. Instytut Nauk Geologicznych Uniwersytetu Jagiellońskiego, Kraków.

Pedersen, T.F., Calvert, S.E., 1990. Anoxia vs. productivity: what controls the formation of organic-carbon-rich sediments and sedimentary rocks? AAPG Bulletin, **74**: 454–466.

Peters, K.E., Cassa, M.R., 1994. Applied source rock geochemistry. AAPG Memoir, **60**: 93–102.

Peters, K.E., Walters, C.C., Moldowan, J.M., 2005. The biomarker Guide; I, Biomarkers and Isotopes in the Environment and Human History. II, Biomarkers and Isotopes in Petroleum Systems and Earth History. 2ed. Cambridge University Press, Cambridge.

Pícha, F.J., Stráník, Z., Krejčí, O., 2006. Geology and hydrocarbon resources of the Outer Western Carpathians and their foreland. AAPG Memoir, **84**: 49–175.

Pickel, W., Kus, J., Flores, D., Kalaitzidis, S., Christanis, K., Cardott, B.J., Misz-Kennan, M., Rodrigues, S., Hentschel, A., Hamor-Vido, M., Crosdale, P., Wagner, N., 2017. Classification of liptinite – ICCP System 1994. International Journal of Coal Geology, **169**: 40–61.

Pupp, M., Bechtel, A., Gratzer, R., Heinrich, M., Kozak, S., Lipiarski, P., Sachsenhofer, R.F., 2018. Depositional environment and petroleum potential of Oligocene rocks in the Waschberg Zone (Austria). Geologica Carpathica, **69**: 410–436.

Stráník, Z., Dvořák, J., Krejčí, O., Müller, P., Přichystal, A., Suk, M., Tomek, Č., 1993. The contact of the North European Epivariscan platform with the West Carpathians. Journal of the Czech Geological Society, **38**: 21–29.

Suaréz-Ruiz, I., Flores, D., Marques, M.M., Martínez-Tarazona, M.R., Pis, J., Rubiera, F., 2006. Geochemistry, mineralogy and technological properties of coals from Rio Maior (Portugal) and Penarroya (Spain) basins. International Journal of Coal Geology, **67**: 171–190.

Sýkorová, I., Pickel, W., Christanis, K., Wolf, M., Taylor, G.H., Flores, D., 2005. Classification of huminite – ICCP System 1994. International Journal of Coal Geology, **62**: 85–106.

Tissot, B.P., Welte, D.H., 1984. Petroleum formation and occurrence. Springer, Berlin, Heidelberg, New York.

Taylor, G.H., Teichmüller, M., Davis, A., Diessel, C.F.K., Littke, R., Robert, P., 1998. Organic Petrology. Gebrüder Borntraeger, Berlin.

Waśkowska, A., Cieszkowski, M., Golonka, J., Kowal-Kasprzyk, J., 2014. Paleocene sedimentary record of ridge geodynamics in Outer Carpathian basins (Subsilesian Unit). Geologica Carpathica, **65**: 35–54.

Więcław, D., 2016. Habitat and hydrocarbon potential of the Kimmeridgian strata in the central part of the Polish Lowlands. Geological Quarterly, **60** (1): 192–210.

Zágoršek, K., Nehyba, S., Tomanová Petrová, P., Hladilová, Š., Bitner, M.A., Doláková, N., Hrabovský, J., Jašková, V., 2012. Local catastrophe caused by tephra input near Přemyslovice (Moravia, Czech Republic) during the Middle Miocene. Geological Quarterly, **56** (2): 269–284.

APPENDIX 1

Results of the TOC content and Rock-Eval analyses of Miocene samples from the Carpathian Foredeep in the Czech Republic

Well ID	Borehole	Segment	Depth [m]	TOC [wt.%]	S1 [mg HC/g rock]	S2 [mg HC/g rock]	T_{max} [°C]	HI [mgHC/gTOC]	PI [-]
32	NP-203	Northern	275	1.12	0.01	0.46	433	41	0.02
33	NP-465	Northern	347	0.69	0.02	0.38	428	55	0.05
34	NP-707	Northern	499	1.03	0.03	0.60	429	58	0.05
34	NP-707	Northern	599	0.89	0.01	0.32	430	36	0.03
34	NP-707	Northern	652	0.91	0.02	0.56	432	62	0.03
35	NP-730	Northern	717	1.67	0.46	0.62	nd	37	0.43
36	NP-895	Northern	53	1.10	0.03	0.52	430	47	0.05
36	NP-895	Northern	60	0.87	0.01	0.38	432	44	0.03
36	NP-895	Northern	63	0.96	0.02	0.38	428	40	0.05
36	NP-895	Northern	95	1.03	0.02	0.50	432	19	0.04
36	NP-895	Northern	97	1.11	0.01	0.48	433	43	0.02
36	NP-895	Northern	104	1.05	0.01	0.46	430	44	0.02
36	NP-895	Northern	106	1.05	0.02	0.44	429	42	0.04
36	NP-895	Northern	139	1.89	0.03	0.76	nd	40	0.04
36	NP-895	Northern	151	0.99	0.01	0.52	430	53	0.02
36	NP-895	Northern	156	1.00	0.02	0.50	432	50	0.04
36	NP-895	Northern	204	0.84	0.01	0.50	429	60	0.02
36	NP-895	Northern	205	0.89	0.02	0.60	432	67	0.03
36	NP-895	Northern	251	0.68	0.02	0.38	431	56	0.05
36	NP-895	Northern	252	0.83	0.01	0.52	432	63	0.02
36	NP-895	Northern	255	1.60	0.01	0.44	432	28	0.02
36	NP-895	Northern	299	0.78	0.02	0.50	432	64	0.04
36	NP-895	Northern	303	0.74	0.02	0.48	432	65	0.04
36	NP-895	Northern	353	0.97	0.01	0.44	432	45	0.02
36	NP-895	Northern	354	1.00	0.00	0.42	432	42	0.00
36	NP-895	Northern	354	0.92	0.01	0.42	433	46	0.02
36	NP-895	Northern	357	0.97	0.02	0.56	429	58	0.03
36	NP-895	Northern	401	1.03	0.02	0.66	432	64	0.03
36	NP-895	Northern	404	1.07	0.01	0.44	432	41	0.02
36	NP-895	Northern	455	1.09	0.01	0.52	432	48	0.02
36	NP-895	Northern	499	1.02	0.01	0.48	432	48	0.02
36	NP-895	Northern	500	1.04	0.01	0.44	432	42	0.02
36	NP-895	Northern	701	0.86	0.01	0.54	427	63	0.02
36	NP-895	Northern	705	0.82	1.00	0.48	429	59	0.68
37	NP-910	Northern	727	0.98	0.03	0.58	432	59	0.05
37	NP-910	Northern	792	1.14	0.02	0.44	429	39	0.04
37	NP-910	Northern	821	0.88	0.04	0.68	429	77	0.06
38	SV-1	Northern	794	0.24	0.14	0.48	422	200	0.23
22	Gottwaldov-1	Central	3525	2.29	0.22	3.04	432	132	0.07

22	Gottwaldov-1	Central	3625	2.30	0.31	4.48	429	194	0.06
22	Gottwaldov-1	Central	3769	0.12	0.06	0.42	437	350	0.13
23	Gottwaldov-2	Central	4240	0.31	0.11	1.14	439	367	0.09
23	Gottwaldov-2	Central	4241	0.74	0.15	1.06	438	143	0.12
23	Gottwaldov-2	Central	4242	0.61	0.19	1.24	437	203	0.13
23	Gottwaldov-2	Central	4242	0.75	0.18	0.70	434	93	0.20
23	Gottwaldov-2	Central	4243	1.04	0.19	0.70	439	67	0.21
23	Gottwaldov-2	Central	4245	0.80	0.15	1.42	437	178	0.10
23	Gottwaldov-2	Central	4296	0.46	0.15	1.76	439	382	0.08
23	Gottwaldov-2	Central	4297	0.49	0.14	0.90	438	183	0.13
23	Gottwaldov-2	Central	4298	0.83	0.21	1.04	437	125	0.17
23	Gottwaldov-2	Central	4299	0.64	0.14	1.74	440	208	0.07
23	Gottwaldov-2	Central	4300	1.33	0.19	0.98	438	73	0.16
23	Gottwaldov-2	Central	4350	0.54	0.18	0.42	437	77	0.30
23	Gottwaldov-2	Central	4350	0.48	0.15	1.24	441	258	0.11
23	Gottwaldov-2	Central	4351	1.17	0.16	0.64	440	54	0.20
23	Gottwaldov-2	Central	4353	0.82	0.28	1.35	445	163	0.17
23	Gottwaldov-2	Central	4415	0.18	0.11	0.32	438	177	0.26
23	Gottwaldov-2	Central	4416	1.25	0.12	0.88	443	175	0.12
23	Gottwaldov-2	Central	4418	0.78	0.30	1.90	440	243	0.14
23	Gottwaldov-2	Central	4484	0.45	0.16	1.06	439	235	0.13
23	Gottwaldov-2	Central	4485	0.96	0.23	1.00	441	104	0.19
23	Gottwaldov-2	Central	4486	0.28	0.02	0.04	445	14	0.33
23	Gottwaldov-2	Central	4487	0.90	0.22	0.98	446	133	0.18
23	Gottwaldov-2	Central	4680	0.67	0.16	0.56	444	83	0.22
23	Gottwaldov-2	Central	4681	1.27	0.26	0.52	441	40	0.33
23	Gottwaldov-2	Central	4682	0.90	0.53	0.80	445	148	0.40
23	Gottwaldov-2	Central	4727	1.27	0.42	3.04	448	239	0.12
23	Gottwaldov-2	Central	4727	2.92	0.96	7.54	442	258	0.11
23	Gottwaldov-2	Central	4730	2.79	1.21	5.72	443	205	0.17
23	Gottwaldov-2	Central	4730	1.18	2.10	8.48	441	341	0.20
39	Gottwaldov-3	Central	3302	0.65	0.09	0.88	433	135	0.09
39	Gottwaldov-3	Central	3402	1.19	0.08	1.70	435	143	0.04
39	Gottwaldov-3	Central	3404	0.31	0.01	0.08	434	26	0.11
39	Gottwaldov-3	Central	3572	1.36	0.05	0.70	435	51	0.07
40	Lubná-11	Central	1577	1.10	0.02	2.10	418	191	0.01
41	Lubná-12	Central	1548	1.20	0.02	1.96	430	163	0.01
25	Lukov-1	Central	2121	1.72	1.25	0.05	na	3	0.96
25	Lukov-1	Central	2176	1.83	1.19	0.08	na	4	0.94
42	Morkovice-2	Central	597	0.70	0.05	1.26	429	180	0.04
42	Morkovice-2	Central	600	0.23	0.02	0.52	430	226	0.04
42	Morkovice-2	Central	786	0.30	0.05	0.84	428	280	0.06
42	Morkovice-2	Central	799	0.72	0.04	0.84	431	116	0.05
42	Morkovice-2	Central	995	0.35	0.03	0.84	432	240	0.03
42	Morkovice-2	Central	1102	1.80	0.08	4.36	426	242	0.02
43	Rousínov-1	Central	683	1.75	0.03	1.94	428	111	0.02

44	Slušovice-1	Central	3094	0.80	0.03	3.15	434	394	0.01
44	Slušovice-1	Central	3095	0.90	0.30	2.03	436	225	0.13
44	Slušovice-1	Central	3201	0.90	0.17	2.27	433	252	0.07
44	Slušovice-1	Central	3202	0.90	0.86	3.65	438	405	0.19
44	Slušovice-1	Central	3318	0.70	0.04	1.37	432	196	0.03
44	Slušovice-1	Central	3318	0.20	0.04	0.22	435	112	0.14
44	Slušovice-1	Central	3318	0.90	0.07	2.19	435	243	0.03
44	Slušovice-1	Central	3319	1.20	4.15	4.15	437	346	0.50
44	Slušovice-1	Central	3457	1.10	0.38	2.33	437	212	0.14
44	Slušovice-1	Central	3457	0.80	0.04	2.06	434	257	0.02
44	Slušovice-1	Central	3550	3.50	3.37	17.71	432	506	0.16
44	Slušovice-1	Central	3573	0.20	0.06	0.51	429	253	0.10
44	Slušovice-1	Central	3573	1.50	0.05	4.97	435	331	0.01
44	Slušovice-1	Central	3576	1.10	0.40	2.95	427	268	0.12
44	Slušovice-1	Central	3698	0.70	0.04	0.69	437	98	0.06
44	Slušovice-1	Central	3698	1.10	0.51	1.62	438	147	0.24
45	Vrbka-1	Central	1495	1.37	0.06	1.30	425	95	0.04
46	Ždánice-25	Central	799	2.50	0.10	9.43	428	377	0.01
47	Ždánice-27	Central	836	3.80	0.59	2.09	418	55	0.22
48	Ždánice-46	Central	780	2.09	1.80	4.18	428	200	0.30
48	Ždánice-46	Central	784	1.54	0.45	2.25	426	146	0.17
49	Ždánice-47	Central	735	5.20	0.50	13.10	420	252	0.04
49	Ždánice-47	Central	760	0.86	0.07	1.03	429	120	0.06
50	Ždánice-53	Central	948	0.59	0.26	0.70	423	118	0.27
50	Ždánice-53	Central	962	1.05	0.14	1.42	422	135	0.09
51	Ždánice-54	Central	750	3.03	0.40	6.39	425	211	0.06
52	Ždánice-55	Central	702	0.61	0.09	0.36	416	59	0.20
52	Ždánice-55	Central	725	0.61	0.03	0.30	422	49	0.09
52	Ždánice-55	Central	750	0.77	0.05	0.45	428	59	0.10
52	Ždánice-55	Central	777	1.67	0.06	1.24	428	74	0.05
53	Ždánice-57	Central	760	9.17	2.20	8.25	413	90	0.21
53	Ždánice-57	Central	760	4.29	0.30	6.01	429	140	0.05
54	Ždánice-58	Central	772	2.28	0.60	1.53	415	67	0.28
54	Ždánice-58	Central	794	2.97	0.27	1.81	426	61	0.13
55	Ždánice-59	Central	748	3.00	1.10	9.93	419	331	0.10
55	Ždánice-59	Central	830	2.56	0.75	3.48	423	136	0.18
56	Ždánice-60	Central	695	0.60	0.23	0.62	425	103	0.27
56	Ždánice-60	Central	730	0.91	0.45	0.67	428	74	0.40
57	Ždánice-66	Central	710	1.75	0.40	2.24	431	128	0.15
57	Ždánice-66	Central	715	2.76	0.20	8.83	422	320	0.02
57	Ždánice-66	Central	720	0.64	0.06	0.98	428	153	0.06
57	Ždánice-66	Central	795	0.53	0.10	0.57	432	107	0.15
58	Brod n. Dyjí-1	Southern	695	1.97	0.10	8.55	431	434	0.01
26	Březí-1	Southern	912	nd	nd	nd	430	nd	nd
27	Březí-2	Southern	1242	nd	nd	nd	421	nd	nd
27	Březí-2	Southern	1296	nd	nd	nd	428	nd	nd

28	Dunajovice-1	Southern	752	nd	nd	nd	430	nd	nd
29	Dunajovice-3	Southern	1121	2.00	0.76	5.10	425	255	0.13
30	Dunajovice-16	Southern	1043	nd	nd	nd	425	nd	nd
59	Mikulov-4	Southern	795	0.65	0.29	0.68	429	104	0.03
59	Mikulov-4	Southern	940	0.77	0.02	0.62	429	80	0.03
59	Mikulov-4	Southern	1055	0.53	0.01	0.23	419	44	0.04
59	Mikulov-4	Southern	1065	1.15	0.02	1.10	427	96	0.02
31	Mušov-2	Southern	81	nd	nd	nd	426	nd	nd
60	Nikolčice-3	Southern	1095	2.90	0.69	7.89	425	272	0.08
61	Pohořelice-1	Southern	500	0.82	0.09	1.42	420	173	0.06

TOC - total Organic Carbon, S1 - volatile hydrocarbon (HC) content, S2 - residual HC generative potential, T_{max} - temperature of the maximum of S2 peak, HI - hydrogen Index, PI - production Index, na – not available, nd – not determined.

APPENDIX 2

Random reflectance of huminite/vitrinite of organic matter in Miocene samples from the Carpathian Foredeep in the Czech Republic

Well ID	Borehole	Segment	Depth [m]	R_r [%]
10	Janovice-8	Northern	1142	0.54
11	Frenštát pod Radhoštěm-13	Northern	777	0.47
12	Frenštát pod Radhoštěm-3	Northern	955	0.51
13	Lhotka-5	Northern	871	0.34
14	NP-547	Northern	962	0.51
15	NP-549	Northern	998	0.46
15	NP-549	Northern	993	0.52
15	NP-549	Northern	994	0.53
15	NP-549	Northern	995	0.54
15	NP-549	Northern	995	0.55
16	NP-779	Northern	179	0.36
17	NP-803	Northern	1035	0.46
17	NP-803	Northern	1035	0.48
17	NP-803	Northern	1034	0.50
17	NP-803	Northern	1028	0.56
18	NP-812	Northern	942	0.39
18	NP-812	Northern	879	0.43
19	NP-818	Northern	910	0.44
20	NP-824	Northern	1002	0.52
21	NP-828	Northern	1353	0.58
26	Březí-1	Southern	912	0.32
27	Březí-2	Southern	1242	0.33
27	Březí-2	Southern	1296	0.43
28	Dunajovice-1	Southern	1024	0.28
29	Dunajovice-3	Southern	1122	0.27
30	Dunajovice-16	Southern	1043	0.41
31	Mušov-2	Southern	801	0.29

Data from the borehole reports